Prepared for submission to JHEP FERMILAB-PUB-18-014-T

Addendum to "Compact Perturbative Expressions for Neutrino Oscillations in Matter"

Peter B. Denton,[a] **Hisakazu Minakata,**[b] **Stephen J. Parke**[c]

[a] *Niels Bohr International Academy, Niels Bohr Institute, University of Copenhagen, Blegdamsvej 17, 2100, Copenhagen, Denmark*

[b] *Instituto Física Teórica, UAM/CSIC, Calle Nicola's Cabrera 13-15, Cantoblanco E-28049 Madrid, Spain. & Research Center for Cosmic Neutrinos, Institute for Cosmic Ray Research, University of Tokyo, Kashiwa, Chiba 277-8582, Japan*

[c] *Theoretical Physics Department, Fermi National Accelerator Laboratory, P. O. Box 500, Batavia, IL 60510, USA*

E-mail: peterbd1@gmail.com, hisakazu.minakata@gmail.com, parke@fnal.gov

Abstract: In this Addendum we rewrite the neutrino mixing angles and mass squared differences in matter given in our original paper, [1], in a notation that is more conventional for the reader. Replacing the usual neutrino mixing angles and mass squared differences in the expressions for the vacuum oscillation probabilities with these matter mixing angles and mass squared differences gives an excellent approximation to the oscillation probabilities in matter. Comparisons for T2K & T2HK, NOvA, T2HKK and DUNE are also given for neutrinos and anti-neutrinos, disappearance and appearance channels and for both normal and inverted orderings.

Keywords: Neutrino Physics, Neutrino Oscillations in Matter, CP violation

This manuscript has been authored by Fermi Research Alliance, LLC under Contract No. DE-AC02-07CH11359 with the U.S. Department of Energy, Office of Science, Office of High Energy Physics.

Contents

1 Introduction

In this Addendum we rewrite the neutrino mixing angles and mass squared differences in matter given in our original paper, [1], in a notation that is more conventional for the reader. Replacing the usual neutrino mixing angles and mass squared differences in the expressions for the vacuum oscillation probabilities with these matter mixing angles and mass squared differences gives an excellent approximation to the oscillation probabilities in matter. Higher orders are also easily calculated and provide several orders of magnitude improvement per order.

In Section 2, we give the approximation to the mixing angles and mass squared difference in matter and discuss how to use these to calculated the oscillation probabilities in matter both at 0th order and 1st order. We also give expansions of the mixing angles and mass squared differences in matter in powers of $(a/\Delta m^2)$. In Section 3, we make a detailed comparison between the exact and the approximate oscillation probabilities in matter for the T2K & T2HK (295 km), NOvA (810 km), T2HKK (1050 km) and DUNE (1300 km) experiments. Section 4 is the Summary.

2 Mixing Angles and Mass Differences in Matter

2.1 Zeroth Order

In this section, a simple and accurate way to evaluate oscillation probabilities, recently shown in [1], is given.[1] Details as to the why's and how's of this method are contained in that paper.

The mixing angles in matter, which we denote by a $\widetilde{\theta}_{13}$ and $\widetilde{\theta}_{12}$ here, can also be calculated in the following way, using $\Delta m^2_{ee} \equiv \cos^2\theta_{12}\Delta m^2_{31} + \sin^2\theta_{12}\Delta m^2_{32}$, as follows[2], see [2]:

$$\cos 2\widetilde{\theta}_{13} = \frac{(\cos 2\theta_{13} - a/\Delta m^2_{ee})}{\sqrt{(\cos 2\theta_{13} - a/\Delta m^2_{ee})^2 + \sin^2 2\theta_{13}}}, \tag{2.1.1}$$

where $a \equiv 2\sqrt{2}G_F N_e E_\nu$ is the standard matter potential, and

$$\cos 2\widetilde{\theta}_{12} = \frac{(\cos 2\theta_{12} - a'/\Delta m^2_{21})}{\sqrt{(\cos 2\theta_{12} - a'/\Delta m^2_{21})^2 \ + \ \sin^2 2\theta_{12}\cos^2(\widetilde{\theta}_{13} - \theta_{13})}}, \tag{2.1.2}$$

where $a' \equiv a\,\cos^2\widetilde{\theta}_{13} + \Delta m^2_{ee}\sin^2(\widetilde{\theta}_{13} - \theta_{13})$ is the θ_{13}-modified matter potential for the 1-2 sector. In these two flavor rotations, both $\widetilde{\theta}_{13}$ and $\widetilde{\theta}_{12}$ are in range $[0, \pi/2]$.

θ_{23} and δ are unchanged in matter for this approximation.

From the neutrino mass squared eigenvalues in matter, given by

$$\begin{aligned}
\widetilde{m^2_3} &= \Delta m^2_{31} + (\,a - a'\,),\\
\widetilde{m^2_2} &= \Delta m^2_{21} + \frac{1}{2}(a' + \Delta\widetilde{m^2}_{21} - \Delta m^2_{21}\,),\\
\widetilde{m^2_1} &= \frac{1}{2}(a' - \Delta\widetilde{m^2}_{21} + \Delta m^2_{21}\,),
\end{aligned} \tag{2.1.3}$$

it is simple to obtain the neutrino mass squared differences in matter, i.e. the Δm^2_{jk} in matter, which we denote by $\Delta\,\widetilde{m^2}_{jk}$, which are given by

$$\begin{aligned}
\Delta\,\widetilde{m^2}_{21} &= \Delta m^2_{21}\,\sqrt{(\cos 2\theta_{12} - a'/\Delta m^2_{21})^2 \ + \ \sin^2 2\theta_{12}\cos^2(\widetilde{\theta}_{13} - \theta_{13})}\ \ ,\\
\Delta\,\widetilde{m^2}_{31} &= \Delta m^2_{31} + (\,a - \frac{3}{2}a'\,) + \frac{1}{2}\left(\,\Delta\widetilde{m^2}_{21} - \Delta m^2_{21}\,\right),\\
\Delta\,\widetilde{m^2}_{32} &= \Delta\,\widetilde{m^2}_{31} - \Delta\,\widetilde{m^2}_{21}.
\end{aligned} \tag{2.1.4}$$

[1] In this note ϕ, ψ and $\Delta\lambda_{jk}$ of [1], are replaced with the more traditional notation $\widetilde{\theta}_{13}$ and $\widetilde{\theta}_{12}$ and $\Delta\,\widetilde{m^2}_{jk}$ respectively.

[2] Vacuum values to be used in calculating Δm^2_{ee}.

Note that the same square root[3] appears in both $\Delta\widetilde{m^2}_{21}$ and $\sin^2\widetilde{\theta}_{12}$. To see that the $\Delta\widetilde{m^2}_{31}$ and $\Delta\widetilde{m^2}_{32}$ have the right asymptotic forms, use the fact that $(\Delta\widetilde{m^2}_{21} - \Delta m^2_{21}) = |a'| + \mathcal{O}(\Delta m^2_{21})$, for $|a| \gg \Delta m^2_{21}$.

In Fig. 1 and Fig. 2 the values of matter potentials, a, a′, sine squared of the matter mixing angles, $\sin^2\widetilde{\theta}_{13}$ and $\sin^2\widetilde{\theta}_{12}$, the matter mass squared eigenvalues, $\widetilde{m^2}_j$, and the matter mass squared differences[4], $\Delta\widetilde{m^2}_{jk}$, as a function of the neutrino energy for a density of 3.0 g.cm^{-3}.

To calculate the oscillation probabilities, to 0th order, use the above $\Delta\widetilde{m^2}_{jk}$ instead of Δm^2_{jk} and replace the vacuum MNS matrix as follows

$$U^0_{MNS} \equiv U_{23}(\theta_{23})\, U_{13}(\theta_{13}, \delta)\, U_{12}(\theta_{12}) \Rightarrow U^M_{MNS} \equiv U_{23}(\theta_{23})\, U_{13}(\,\widetilde{\theta}_{13}, \delta)\, U_{12}(\widetilde{\theta}_{12}).$$

That is, replace

$$\begin{aligned} \Delta m^2_{jk} &\to \Delta\widetilde{m^2}_{jk} \\ \theta_{13} &\to \widetilde{\theta}_{13} \\ \theta_{12} &\to \widetilde{\theta}_{12}, \end{aligned} \tag{2.1.5}$$

θ_{23} and δ remain unchanged, it is that simple. We call this the 0th order DMP approximation.

These expressions are valid for both NO, $\Delta m^2_{ee} > 0$ and IO, $\Delta m^2_{ee} < 0$. For anti-neutrinos, just change the sign of a and δ. Our expansion parameter is

$$\left| \sin(\widetilde{\theta}_{13} - \theta_{13})\ \sin\theta_{12}\cos\theta_{12}\ \frac{\Delta m^2_{21}}{\Delta m^2_{ee}} \right| \leq 0.015, \tag{2.1.6}$$

which is small and vanishes in vacuum, so that our perturbation theory reproduces the vacuum oscillation probabilities exactly.

If $P_{\nu_\alpha\to\nu_\beta}(\Delta m^2_{31}, \Delta m^2_{21}, \theta_{13}, \theta_{12}, \theta_{23}, \delta)$ is the oscillation probability in vacuum then $P_{\nu_\alpha\to\nu_\beta}(\Delta\widetilde{m^2}_{31}, \Delta\widetilde{m^2}_{21}, \widetilde{\theta}_{13}, \widetilde{\theta}_{12}, \theta_{23}, \delta)$ is the oscillation probability in matter, i.e. use the same function but replace the mass squared differences and mixing angles with the matter values given in eq. 2.1.1 - 2.1.4. The resulting oscillation probabilities are identical to the zeroth order approximation given in Denton, Minakata and Parke, [1].

2.2 Higher Orders

If the 0th order is not accurate enough, going to 1st order is simple and gives another two orders of magnitude in accuracy. First the $\Delta\widetilde{m^2}_{jk}$ remain unchanged but the mixing matrix is modified by

$$U^M_{MNS} \Rightarrow V \equiv U^M_{MNS}(1 + W_1), \tag{2.2.1}$$

[3] If $a = 0$, then $\widetilde{\theta}_{13} = \theta_{13}$ and since $a' = 0$ then $\widetilde{\theta}_{12} = \theta_{12}$ and both $\sqrt{\cdots} = 1$, also $\Delta\widetilde{m^2}_{jk} = \Delta m^2_{jk}$ for all (j,k) as required. The identity $s^2_\theta = (1 - \cos 2\theta)/2$ is useful for calculating both s_θ and c_θ.

[4] For NO, we plot $(jk) = (31), (32)$ & (21), whereas for IO we plot $(jk) = (13), (23)$ & (21), this way all Δm^2's plotted are positive.

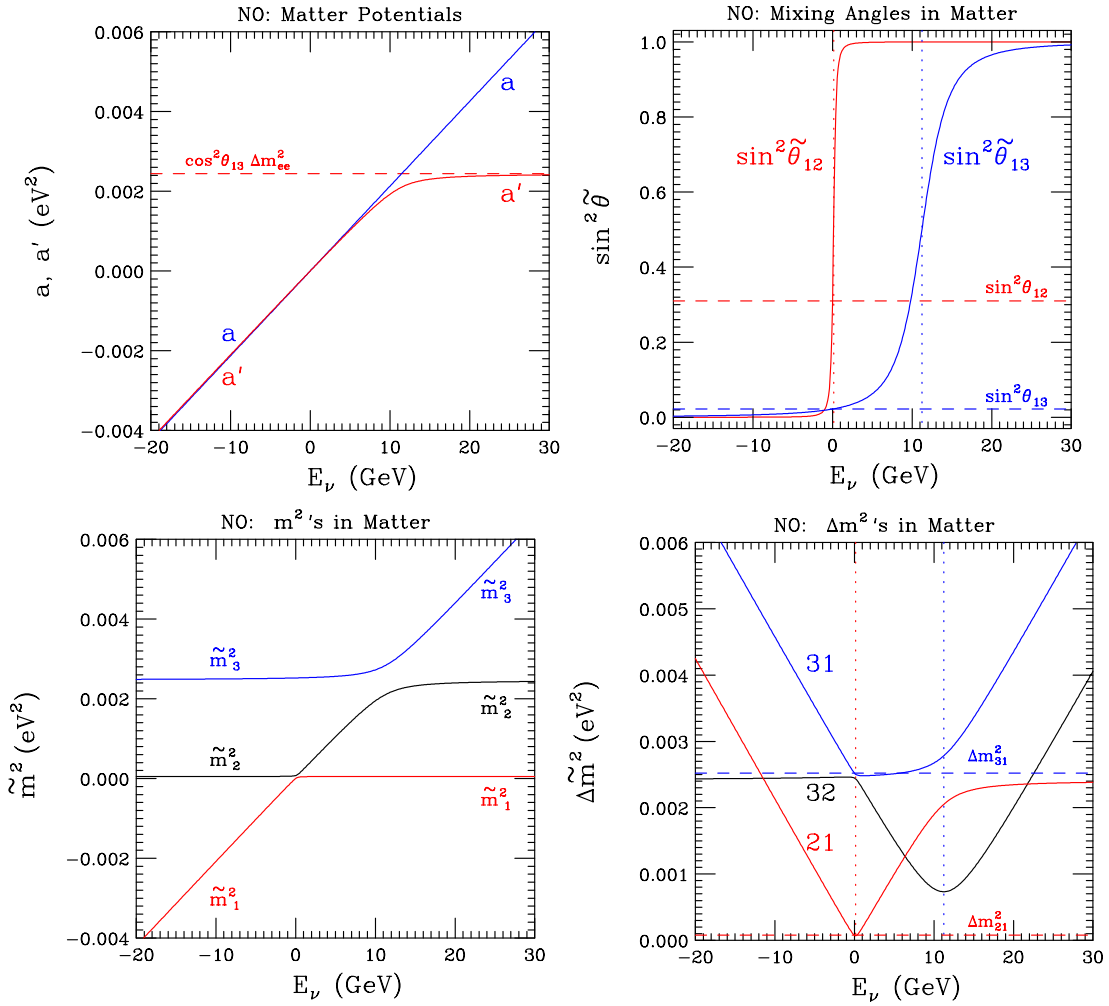

Figure 1: In the normal ordering (NO): Top left, the matter potentials, a and a', top right, sine squared of mixing angles in matter, $\sin^2\widetilde{\theta}_{jk}$, bottom left, the mass squared eigenvalues in matter, $\widetilde{m^2}_j$, and bottom right, the mass squared differences in matter, $\Delta\widetilde{m^2}_{jk}$. $E_\nu \geq 0$ ($E_\nu \leq 0$) is for neutrinos (anti-neutrinos). $E_\nu = 0$ is the vacuum values for both neutrinos and anti-neutrinos.

where the matrix W_1 is given by

$$W_1 = \sin(\widetilde{\theta}_{13} - \theta_{13})\; s_{12}c_{12}\; \Delta m^2_{21}$$

$$\begin{pmatrix} 0 & 0 & -\widetilde{s}_{12}\, e^{-i\delta}/\Delta\widetilde{m^2}_{31} \\ 0 & 0 & +\widetilde{c}_{12}\, e^{-i\delta}/\;\Delta\widetilde{m^2}_{32} \\ +\widetilde{s}_{12}\, e^{+i\delta}/\Delta\widetilde{m^2}_{31} & -\widetilde{c}_{12}\, e^{+i\delta}/\Delta\widetilde{m^2}_{32} & 0 \end{pmatrix}. \quad (2.2.2)$$

where $\widetilde{s}_{12} = \sin\widetilde{\theta}_{12}$ and $\widetilde{c}_{12} = \cos\widetilde{\theta}_{12}$ etc. The $\Delta\widetilde{m^2}_{jk}$ and the V-mixing matrix can be used to calculate the oscillation probabilities and improves the accuracy by two orders of

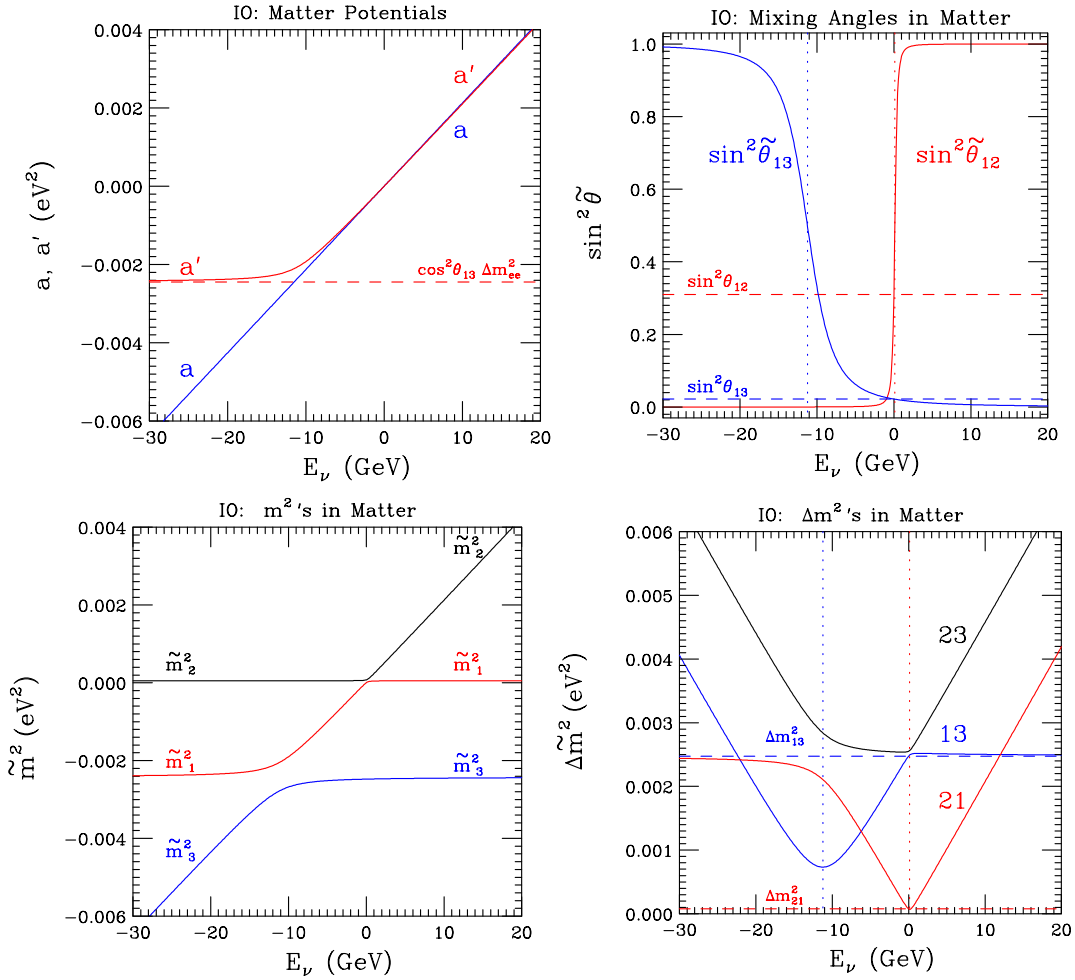

Figure 2: In the inverted ordering (IO): Top left, the matter potentials, a and a', top right, sine squared of mixing angles in matter, $\sin^2\widetilde{\theta}_{jk}$, bottom left, the mass squared eigenvalues in matter, $\widetilde{m^2}_j$, and bottom right, the mass squared differences in matter, $\Delta\,\widetilde{m^2}_{jk}$. $E_\nu \geq 0$ ($E_\nu \leq 0$) is for neutrinos (anti-neutrinos). $E_\nu = 0$ is the vacuum values for both neutrinos and anti-neutrinos.

magnitude. We call this the 1st order DMP approximation. The next highest order, 2nd order, is also discussed in [1].

2.3 Expansions in $a/\Delta m^2$

If $|a| \ll |\Delta m^2_{ee}|$, that is when $E_\nu \ll 11\,\big(\,\rho\,/\,3\ \mathrm{g\,cm^{-3}}\big)$ GeV, we have,

$$\begin{aligned}
\sin^2\widetilde{\theta}_{13} &\approx s^2_{13}\Big[1 + 2c^2_{13}(a/\Delta m^2_{ee}) + 3(c^2_{13} - s^2_{13})c^2_{13}(a/\Delta m^2_{ee})^2 + \mathcal{O}(a/\Delta m^2_{ee})^3)\Big] \\
\sin^2(\widetilde{\theta}_{13} - \theta_{13}) &\approx s^2_{13}c^2_{13}(a/\Delta m^2_{ee})^2\Big[1 + 2(c^2_{13} - s^2_{13})(a/\Delta m^2_{ee}) + \mathcal{O}(a/\Delta m^2_{ee})^2\Big] \qquad (2.3.1) \\
a' &\approx ac^2_{13}\Big[1 - s^2_{13}(a/\Delta m^2_{ee}) - s^2_{13}(c^2_{13} - s^2_{13})(a/\Delta m^2_{ee})^2 + \mathcal{O}(a/\Delta m^2_{ee})^3\Big]
\end{aligned}$$

up to $\mathcal{O}(a/\Delta m^2_{ee})^2$. The expansion for a' can be used to calculate $\Delta\widetilde{m^2}_{31}$ as follows,

$$\Delta\widetilde{m^2}_{31} = \begin{cases} \Delta m^2_{31} + \ (\,a - a'\,) + \frac{1}{2}\,\Big[\,\Delta\widetilde{m^2}_{21} - \Delta m^2_{21} - a'\,\Big]\,, & a, a' > 0 \\ \Delta m^2_{31} + (\,a - 2a'\,) + \frac{1}{2}\,\Big[\,\Delta\widetilde{m^2}_{21} - \Delta m^2_{21} + a'\,\Big]\,, & a, a' < 0 \end{cases} \qquad (2.3.2)$$

where the quantities in $[\cdots]$ is of $\mathcal{O}(\Delta m^2_{21})$ for all values of E_ν.

As can be seen from Fig. 1 and Fig. 2, both $\Delta\widetilde{m^2}_{21}$ and $\sin^2\widetilde{\theta}_{12}$ make rapid changes in +150 MeV region. Well away from this region, when $|a| \gg |\Delta m^2_{21}|$, that is $E_\nu \gg 150\,\big(\,\rho\,/\,3\ \mathrm{g\,cm^{-3}}\big)$ MeV, we can write

$$\Delta\widetilde{m^2}_{21} \approx |\,a' - \Delta m^2_{21}\cos 2\theta_{12}\,|\,, \qquad (2.3.3)$$

for $|\ a' - \Delta m^2_{21}\cos 2\theta_{12}\,| \gg \Delta m^2_{21}$. This can be used to obtain the asymptotic values for neutrino mass squareds in matter, which agree with the values given in [1].

3 Oscillation Probabilities

3.1 Comparisons

Neutrino parameters relevant for oscillations:

$$\begin{aligned}
\Delta m^2_{ee} = \pm\ 2.5\times10^{-3}\ \mathrm{eV}^2,\ \ \Delta m^2_{21} = +\ 7.5\times10^{-5}\ \mathrm{eV}^2 \\
\sin^2\theta_{12} = 0.31,\ \ \sin^2\theta_{23} = 0.43 \\
\sin^2\theta_{13} = 0.022,\ \ \delta = -72^\circ = -2\pi/5 \qquad (3.1.1)
\end{aligned}$$

Where $\Delta m^2_{ee} > 0$ gives a normal ordering (NO) neutrino spectrum and $\Delta m^2_{ee} < 0$ for inverted ordering (IO). Note we have avoided the special points: $\theta_{23} = \pi/4$ as well as $\delta = 0, \pm\pi/2, \pi$, so as not to overestimate the precision.

We consider four experimental setups: to be comprehensive, the energy windows are chosen to be wider than that accessible for a particular experiment.

- T2K [4] & T2HK [5]: with baseline, L = 295 km, neutrino energy $0.2 < E_\nu/\mathrm{GeV} < 3.0$,
  and density, $\rho = 2.3$ g.cm^{-3}. See Fig. 3, 4.

- NOvA [6]: with baseline, L = 810 km, neutrino energy $0.6 < E_\nu/\text{GeV} < 4.0$, and density, $\rho = 3.0$ g.cm^{-3}. See Fig. 5, 6.
- T2HKK [7]: with baseline, L = 1050 km, neutrino energy $0.3 < E_\nu/\text{GeV} < 5.0$, and density, $\rho = 3.0$ g.cm^{-3}. See Fig. 7, 8.
- DUNE [8]: with baseline, L = 1300 km, neutrino energy $0.5 < E_\nu/\text{GeV} < 7.0$, and density, $\rho = 3.0$ g.cm^{-3}. See Fig. 9, 10.

In these figures we have considered the channels ν_μ disappearance and ν_e appearance for neutrinos and anti-neutrinos and for both NO and IO. Each figure consists of three panels: the top panel is the exact oscillation probabilities in matter from Zaglauer and Schwarzer, [3], the 0th order DMP approximation, [1] as well as the exact vacuum oscillation probability. In the disappearance channel the difference between the three probabilities is less than the thickness of the lines. *In the appearance channel, the difference between exact and 0th order DMP probabilities is less than the thickness of the lines.* The middle (bottom) panel shows the difference (fractional difference) between

1. the exact, [3], and vacuum oscillation probabilities (black dots),
2. the exact and the 0th order DMP approximation, [1], (solid red),
3. the exact and the 1st order DMP approximation, [1], (solid magenta).

In the fractional differences, the denominator is the average of the two probabilities being compared. In Fig, 3 to Fig. 10, the "dips" in middle and bottom panels appear when ΔP changes sign.

In Table 1, we give the maximum difference and fractional difference of the 0th order approximation to the exact probability.

	T2K/HK	NOvA	T2HKK	DUNE
max ΔP	10^{-5}	10^{-4}	10^{-4}	10^{-4}
max $\Delta P/P$	10^{-3}	10^{-3}	$10^{-2.5}$	10^{-2}

Table 1: The maximum ΔP and $\Delta P/P$ at 0th order in the DMP approximation. The largest fraction difference occurs at oscillation maximum for ν_μ disappearance channel, where the oscillation probability is a few %. None of the experiments included here, T2K & T2HK, NOvA, T2HKK and DUNE will be within an order a magnitude of being sensitive to any of these differences.

4 Summary

In summary, the simple 0th order approximation of DMP, [1], is sufficiently accurate for all of the accelerator based neutrino oscillation experiments operating or planned: T2K & T2HK, NOvA, T2HKK and DUNE. First order, which is also simple to implement, improves the accuracy by a further two orders of magnitude.

5 Acknowledgements

This manuscript has been authored by Fermi Research Alliance, LLC under Contract No. DE-AC02-07CH11359 with the U.S. Department of Energy, Office of Science, Office of High Energy Physics.

This project has received funding/support from the European Union's Horizon 2020 research and innovation programme under the Marie Sklodowska-Curie grant agreement No 690575. This project has received funding/support from the European Union's Horizon 2020 research and innovation programme under the Marie Sklodowska-Curie grant agreement No 674896.

HM is supported by Instituto Física Teórica, UAM/CSIC in Madrid, via "Theoretical challenges of new high energy, astro and cosmo experimental data" project, Ref: 201650E082.

PBD acknowledges support from the Villum Foundation (Project No. 13164) and the Danish National Research Foundation (DNRF91 and Grant No. 1041811001).

References

[1] P. B. Denton, H. Minakata and S. J. Parke,
"Compact Perturbative Expressions For Neutrino Oscillations in Matter,"
JHEP **1606**, 051 (2016) doi:10.1007/JHEP06(2016)051 [arXiv:1604.08167 [hep-ph]].

[2] S. J. Parke, P. B. Denton and H. Minakata,
"Analytic Neutrino Oscillation Probabilities in Matter: Revisited,"
arXiv:1801.00752 [hep-ph].

S.J. Parke and M.D. Messier,
"Cross Check of NOvA Oscillation Probabilities"
(1/12/2018), NOVA-doc-25833, FERMILAB-FN-1049,
http://doi.org/10.5281/zenodo.1146747

[3] H. W. Zaglauer and K. H. Schwarzer,
"The Mixing Angles in Matter for Three Generations of Neutrinos and the MSW Mechanism,"
Z. Phys. C **40** (1988) 273.

[4] K. Abe *et al.* [T2K Collaboration],
"The T2K Experiment,"
Nucl. Instrum. Meth. A **659**, 106 (2011) doi:10.1016/j.nima.2011.06.067 [arXiv:1106.1238 [physics.ins-det]].

[5] K. Abe *et al.* [Hyper-Kamiokande Proto- Collaboration],
"Physics potential of a long-baseline neutrino oscillation experiment using a J-PARC neutrino beam and Hyper-Kamiokande,"
PTEP **2015**, 053C02 (2015) doi:10.1093/ptep/ptv061 [arXiv:1502.05199 [hep-ex]].

[6] D. S. Ayres *et al.* [NOvA Collaboration],
"NOvA: Proposal to Build a 30 Kiloton Off-Axis Detector to Study $\nu_\mu \to \nu_e$ Oscillations in the NuMI Beamline,"
hep-ex/0503053.

[7] K. Abe *et al.* [Hyper-Kamiokande proto- Collaboration],
"Physics Potentials with the Second Hyper-Kamiokande Detector in Korea,"
arXiv:1611.06118 [hep-ex].

[8] R. Acciarri *et al.* [DUNE Collaboration],
"Long-Baseline Neutrino Facility (LBNF) and Deep Underground Neutrino Experiment (DUNE) : Volume 2: The Physics Program for DUNE at LBNF,"
arXiv:1512.06148 [physics.ins-det].

$\Delta P = |P^{ex}_{mat} - P_{vac}|$ $\Delta P = |P^{ex}_{mat} - P^{0th}_{appx}|$ $\Delta P = |P^{ex}_{mat} - P^{1st}_{appx}|$

$\overline{P} = \frac{1}{2}(P^{ex}_{mat} + P_{vac})$ $\overline{P} = \frac{1}{2}(P^{ex}_{mat} + P^{0th}_{appx})$ $\overline{P} = \frac{1}{2}(P^{ex}_{mat} + P^{1st}_{appx})$

T2HKK (1050 km)

T2K & T2HK (295 km)

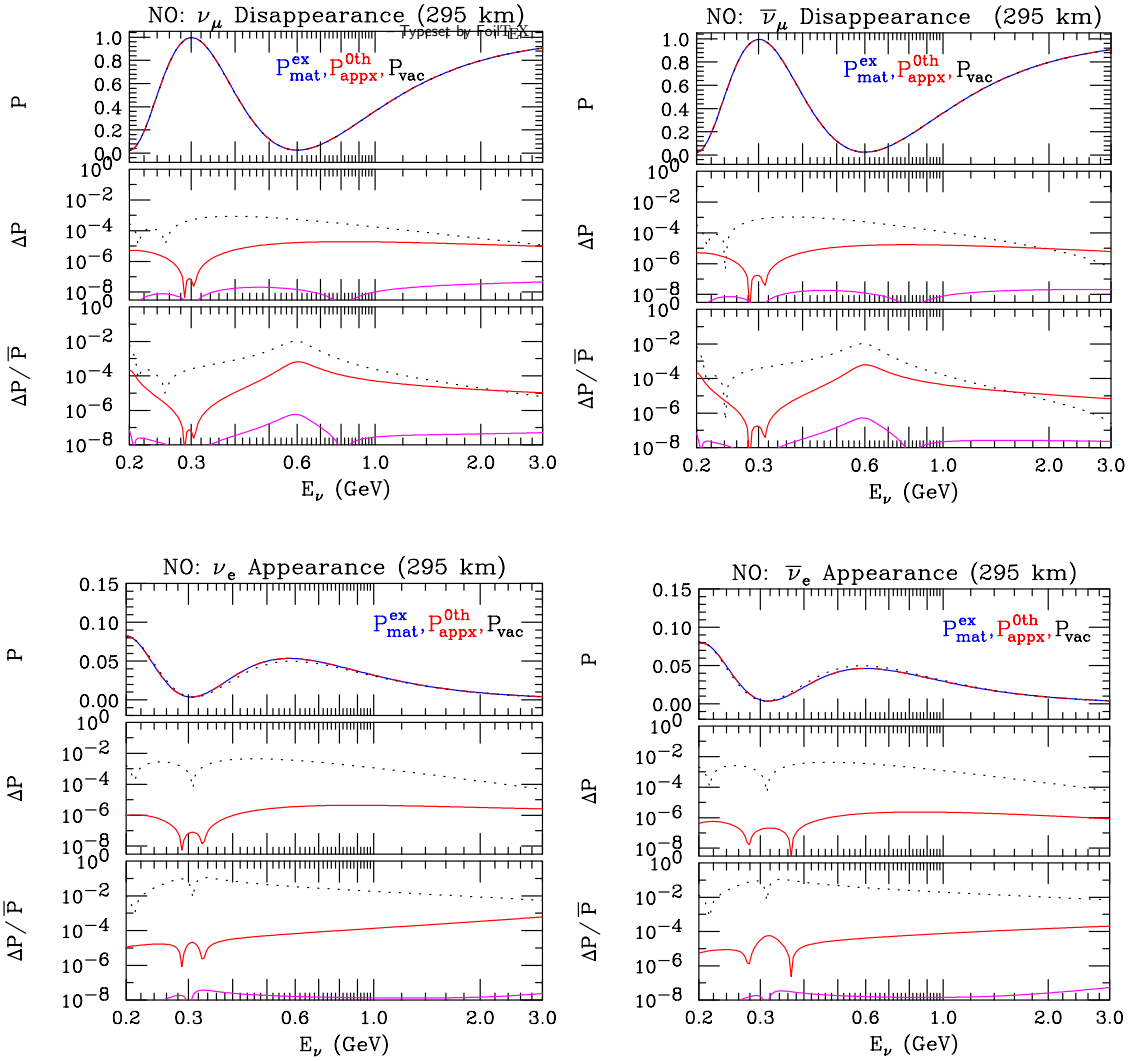

Top panel: P^{ex}_{mat}, P^{0th}_{appx} and P_{vac}

Middle and bottom panels:

black dotted lines	red solid lines	magenta solid lines
$\Delta P = \lvert P^{ex}_{mat} - P_{vac}\rvert$	$\Delta P = \lvert P^{ex}_{mat} - P^{0th}_{appx}\rvert$	$\Delta P = \lvert P^{ex}_{mat} - P^{1st}_{appx}\rvert$
$\overline{P} = \frac{1}{2}(P^{ex}_{mat} + P_{vac})$	$\overline{P} = \frac{1}{2}(P^{ex}_{mat} + P^{0th}_{appx})$	$\overline{P} = \frac{1}{2}(P^{ex}_{mat} + P^{1st}_{appx})$

Figure 3: T2K/HK, for normal ordering (NO): Top Left figure is ν_μ disappearance, Top Right figure is $\bar{\nu}_\mu$ disappearance, Bottom Left figure is $\nu_\mu \to \nu_e$ appearance, and Bottom Right is $\bar{\nu}_\mu \to \bar{\nu}_e$ appearance. In each figure, the top panel is exact oscillation probability in matter, P^{ex}_{mat} (blue dashes) from [3], the zeroth order DMP approximation, P^{0th}_{appx} (red dashes) from [1] and the vacuum oscillation probability, P_{vac} (black dots). The Middle panel is difference between exact oscillation probabilities in matter and vacuum (black dots), and the difference between exact and 0th DMP approximation (solid red) and exact and 1st DMP approximation (solid magenta) approximations. Bottom panel is similar to middle panel but plotting the fractional differences, $\Delta P/\overline{P}$. The density use is 2.3 g.cm^{-3}.

$\Delta P = |P^{ex}_{mat} - P_{vac}|$ $\Delta P = |P^{ex}_{mat} - P^{0th}_{appx}|$ $\Delta P = |P^{ex}_{mat} - P^{1st}_{appx}|$

$\overline{P} = \frac{1}{2}(P^{ex}_{mat} + P_{vac})$ $\overline{P} = \frac{1}{2}(P^{ex}_{mat} + P^{0th}_{appx})$ $\overline{P} = \frac{1}{2}(P^{ex}_{mat} + P^{1st}_{appx})$

T2HKK (1050 km)

T2K & T2HK (295 km)

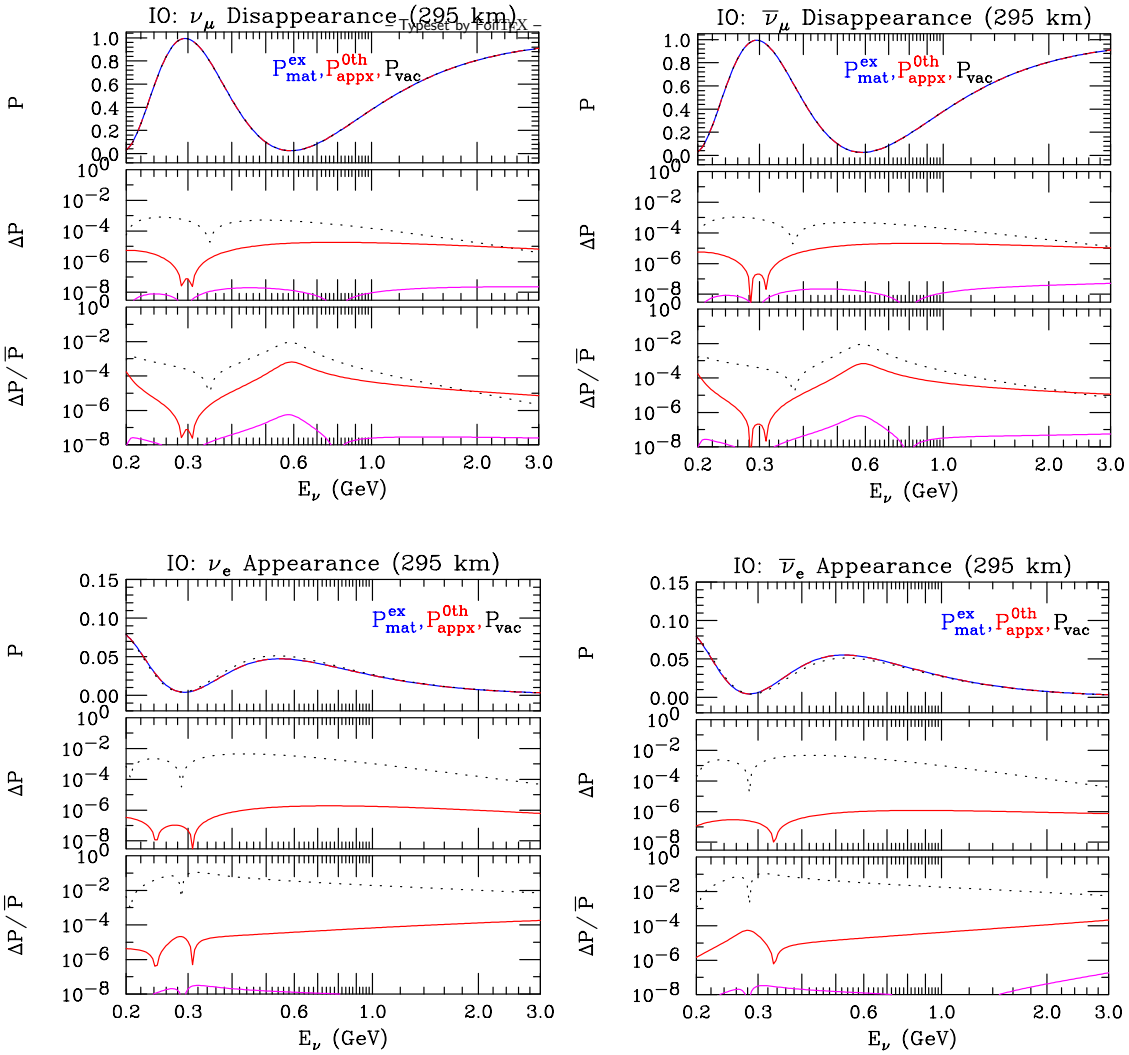

Top panel: P^{ex}_{mat}, P^{0th}_{appx} and P_{vac}

Middle and bottom panels:

black dotted lines	red solid lines	magenta solid lines
$\Delta P = \lvert P^{ex}_{mat} - P_{vac}\rvert$	$\Delta P = \lvert P^{ex}_{mat} - P^{0th}_{appx}\rvert$	$\Delta P = \lvert P^{ex}_{mat} - P^{1st}_{appx}\rvert$
$\overline{P} = \frac{1}{2}(P^{ex}_{mat} + P_{vac})$	$\overline{P} = \frac{1}{2}(P^{ex}_{mat} + P^{0th}_{appx})$	$\overline{P} = \frac{1}{2}(P^{ex}_{mat} + P^{1st}_{appx})$

Figure 4: T2K/HK, for inverted ordering (IO): Top Left figure is ν_μ disappearance, Top Right figure is $\bar{\nu}_\mu$ disappearance, Bottom Left figure is $\nu_\mu \to \nu_e$ appearance, and Bottom Right is $\bar{\nu}_\mu \to \bar{\nu}_e$ appearance. In each figure, the top panel is exact oscillation probability in matter, P^{ex}_{mat} (blue dashes) from [3], the zeroth order DMP approximation, P^{0th}_{appx} (red dashes) from [1] and the vacuum oscillation probability, P_{vac} (black dots). The Middle panel is difference between exact oscillation probabilities in matter and vacuum (black dots), and the difference between exact and 0th DMP approximation (solid red) and exact and 1st DMP approximation (solid magenta) approximations. Bottom panel is similar to middle panel but plotting the fractional differences, $\Delta P/\overline{P}$. The density use is 2.3 g.cm^{-3}.

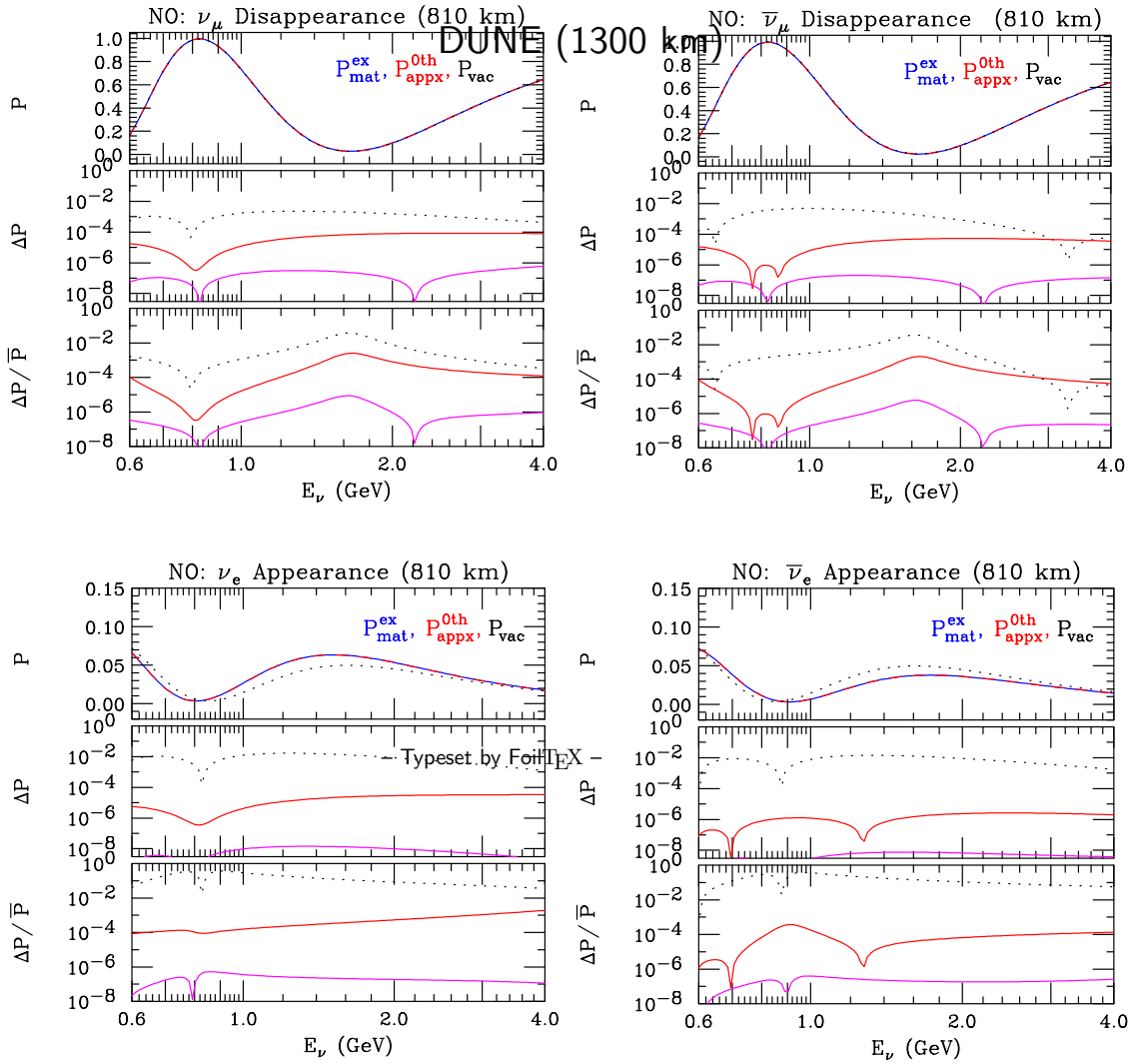

Top panel: P^{ex}_{mat}, P^{0th}_{appx} and P_{vac}

Middle and bottom panels:

black dotted lines	red solid lines	magenta solid lines
$\Delta P = \lvert P^{ex}_{mat} - P_{vac}\rvert$	$\Delta P = \lvert P^{ex}_{mat} - P^{0th}_{appx}\rvert$	$\Delta P = \lvert P^{ex}_{mat} - P^{1st}_{appx}\rvert$
$\overline{P} = \frac{1}{2}(P^{ex}_{mat} + P_{vac})$	$\overline{P} = \frac{1}{2}(P^{ex}_{mat} + P^{0th}_{appx})$	$\overline{P} = \frac{1}{2}(P^{ex}_{mat} + P^{1st}_{appx})$

Figure 5: NOvA, for normal ordering (NO): Top Left figure is ν_μ disappearance, Top Right figure is $\bar{\nu}_\mu$ disappearance, Bottom Left figure is $\nu_\mu \to \nu_e$ appearance, and Bottom Right is $\bar{\nu}_\mu \to \bar{\nu}_e$ appearance. In each figure, the top panel is exact oscillation probability in matter, P^{ex}_{mat} (blue dashes) from [3], the zeroth order DMP approximation, P^{0th}_{appx} (red dashes) from [1] and the vacuum oscillation probability, P_{vac} (black dots). The Middle panel is difference between exact oscillation probabilities in matter and vacuum (black dots), and the difference between exact and 0th DMP approximation (solid red) and exact and 1st DMP approximation (solid magenta) approximations. Bottom panel is similar to middle panel but plotting the fractional differences, $\Delta P/\overline{P}$. The density use is 3.0 g.cm^{-3}.

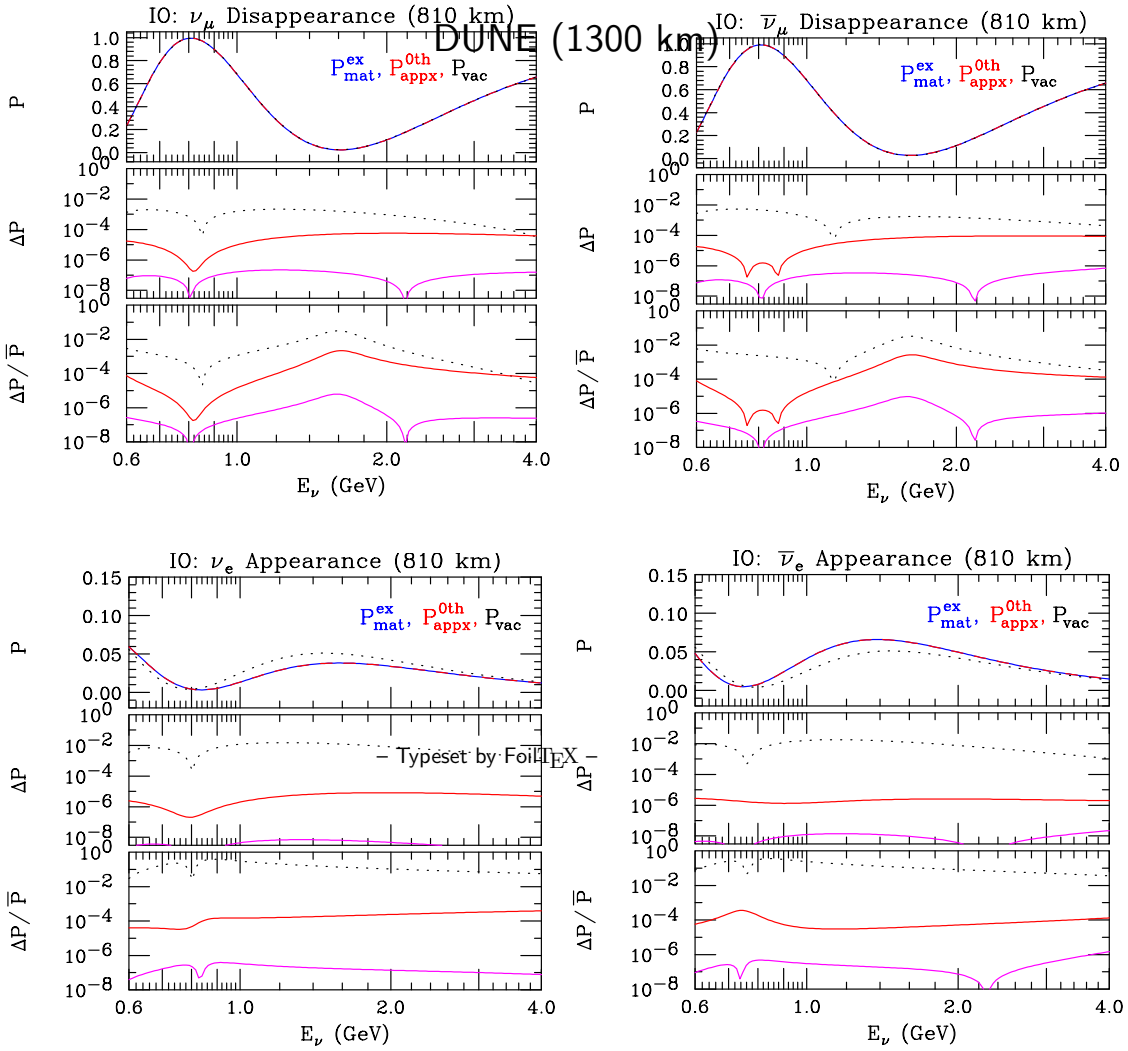

Top panel: P^{ex}_{mat}, P^{0th}_{appx} and P_{vac}

Middle and bottom panels:

black dotted lines	red solid lines	magenta solid lines
$\Delta P = \lvert P^{ex}_{mat} - P_{vac}\rvert$	$\Delta P = \lvert P^{ex}_{mat} - P^{0th}_{appx}\rvert$	$\Delta P = \lvert P^{ex}_{mat} - P^{1st}_{appx}\rvert$
$\overline{P} = \frac{1}{2}(P^{ex}_{mat} + P_{vac})$	$\overline{P} = \frac{1}{2}(P^{ex}_{mat} + P^{0th}_{appx})$	$\overline{P} = \frac{1}{2}(P^{ex}_{mat} + P^{1st}_{appx})$

Figure 6: NOvA, for inverted ordering (IO): Top Left figure is ν_μ disappearance, Top Right figure is $\bar{\nu}_\mu$ disappearance, Bottom Left figure is $\nu_\mu \to \nu_e$ appearance, and Bottom Right is $\bar{\nu}_\mu \to \bar{\nu}_e$ appearance. In each figure, the top panel is exact oscillation probability in matter, P^{ex}_{mat} (blue dashes) from [3], the zeroth order DMP approximation, P^{0th}_{appx} (red dashes) from [1] and the vacuum oscillation probability, P_{vac} (black dots). The Middle panel is difference between exact oscillation probabilities in matter and vacuum (black dots), and the difference between exact and 0th DMP approximation (solid red) and exact and 1st DMP approximation (solid magenta) approximations. Bottom panel is similar to middle panel but plotting the fractional differences, $\Delta P/\overline{P}$. The density use is 3.0 g.cm^{-3}.

$\Delta P = |P^{ex}_{mat} - P_{vac}|$ $\Delta P = |P^{ex}_{mat} - P^{0th}_{appx}|$ $\Delta P = |P^{ex}_{mat} -$

$\overline{P} = \frac{1}{2}(P^{ex}_{mat} + P_{vac})$ $\overline{P} = \frac{1}{2}(P^{ex}_{mat} + P^{0th}_{appx})$ $\overline{P} = \frac{1}{2}(P^{ex}_{mat} +$

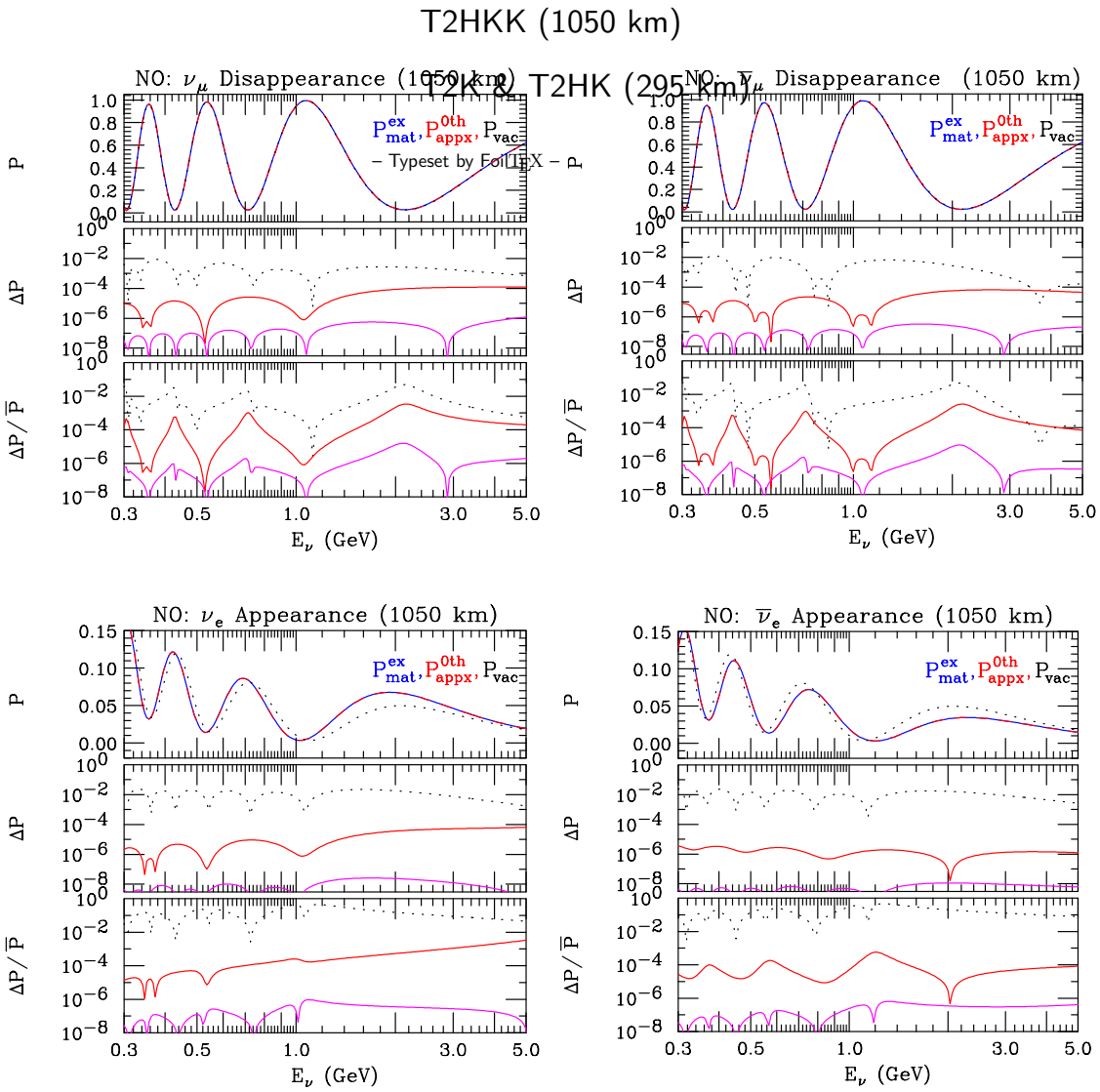

Top panel: P^{ex}_{mat}, P^{0th}_{appx} and P_{vac}

Middle and bottom panels:

black dotted lines	red solid lines	magenta solid lines
$\Delta P = \lvert P^{ex}_{mat} - P_{vac}\rvert$	$\Delta P = \lvert P^{ex}_{mat} - P^{0th}_{appx}\rvert$	$\Delta P = \lvert P^{ex}_{mat} - P^{1st}_{appx}\rvert$
$\overline{P} = \frac{1}{2}(P^{ex}_{mat} + P_{vac})$	$\overline{P} = \frac{1}{2}(P^{ex}_{mat} + P^{0th}_{appx})$	$\overline{P} = \frac{1}{2}(P^{ex}_{mat} + P^{1st}_{appx})$

Figure 7: T2HKK, for normal ordering (NO): Top Left figure is ν_μ disappearance, Top Right figure is $\bar{\nu}_\mu$ disappearance, Bottom Left figure is $\nu_\mu \to \nu_e$ appearance, and Bottom Right is $\bar{\nu}_\mu \to \bar{\nu}_e$ appearance. In each figure, the top panel is exact oscillation probability in matter, P^{ex}_{mat} (blue dashes) from [3], the zeroth order DMP approximation, P^{0th}_{appx} (red dashes) from [1] and the vacuum oscillation probability, P_{vac} (black dots). The Middle panel is difference between exact oscillation probabilities in matter and vacuum (black dots), and the difference between exact and 0th DMP approximation (solid red) and exact and 1st DMP approximation (solid magenta) approximations. Bottom panel is similar to middle panel but plotting the fractional differences, $\Delta P/\overline{P}$. The density use is 3.0 g.cm^{-3}.

$\Delta P = |P^{ex}_{mat} - P_{vac}|$ $\Delta P = |P^{ex}_{mat} - P^{0th}_{appx}|$ $\Delta P = |P^{ex}_{mat} -$

$\overline{P} = \frac{1}{2}(P^{ex}_{mat} + P_{vac})$ $\overline{P} = \frac{1}{2}(P^{ex}_{mat} + P^{0th}_{appx})$ $\overline{P} = \frac{1}{2}(P^{ex}_{mat} +$

T2HKK (1050 km)

T2K & T2HK (295 km)

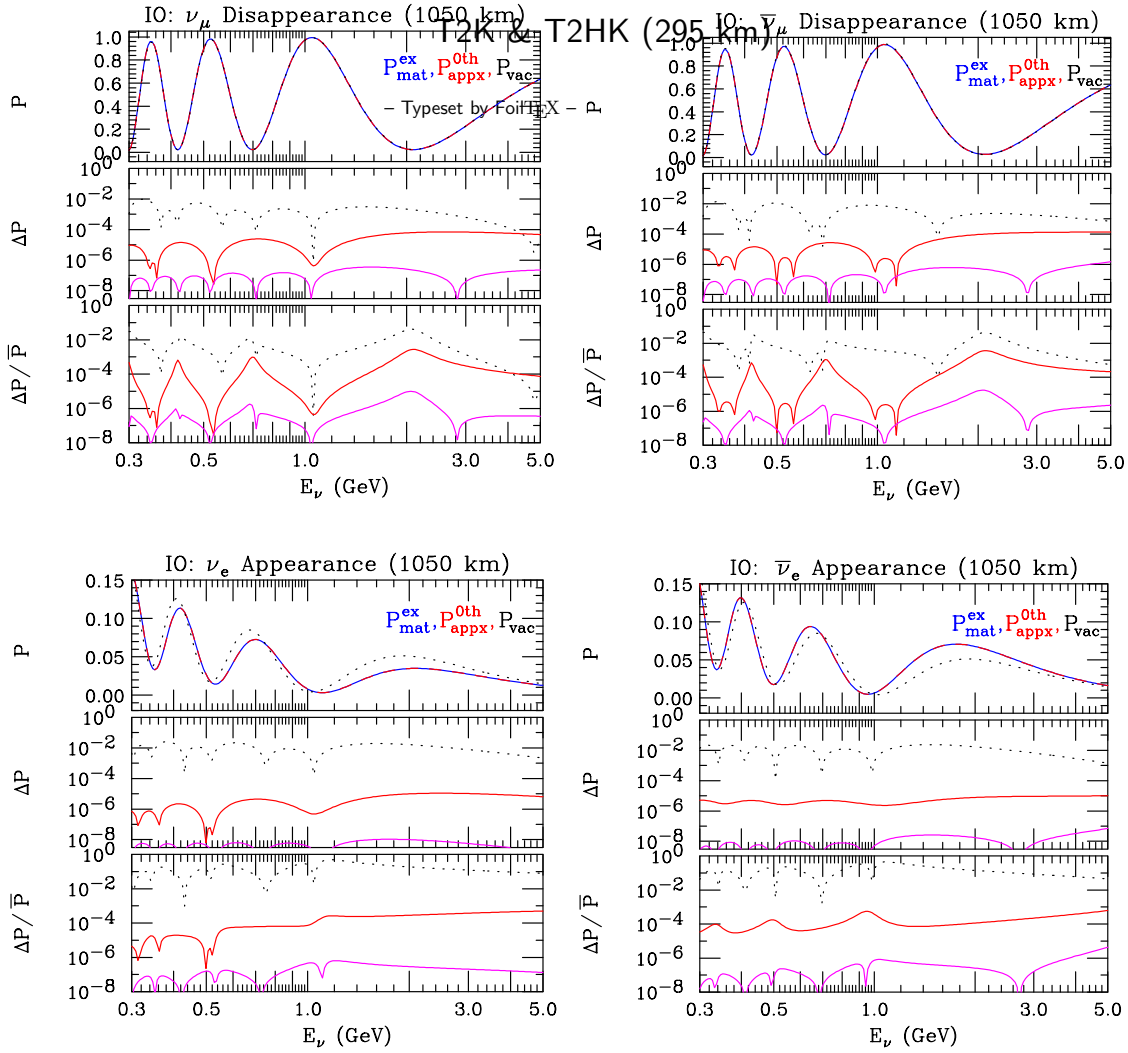

Top panel: P^{ex}_{mat}, P^{0th}_{appx} and P_{vac}

Middle and bottom panels:

black dotted lines	red solid lines	magenta solid lines
$\Delta P = \lvert P^{ex}_{mat} - P_{vac}\rvert$	$\Delta P = \lvert P^{ex}_{mat} - P^{0th}_{appx}\rvert$	$\Delta P = \lvert P^{ex}_{mat} - P^{1st}_{appx}\rvert$
$\overline{P} = \frac{1}{2}(P^{ex}_{mat} + P_{vac})$	$\overline{P} = \frac{1}{2}(P^{ex}_{mat} + P^{0th}_{appx})$	$\overline{P} = \frac{1}{2}(P^{ex}_{mat} + P^{1st}_{appx})$

Figure 8: T2HKK, for inverted ordering (IO): Top Left figure is ν_μ disappearance, Top Right figure is $\bar{\nu}_\mu$ disappearance, Bottom Left figure is $\nu_\mu \to \nu_e$ appearance, and Bottom Right is $\bar{\nu}_\mu \to \bar{\nu}_e$ appearance. In each figure, the top panel is exact oscillation probability in matter, P^{ex}_{mat} (blue dashes) from [3], the zeroth order DMP approximation, P^{0th}_{appx} (red dashes) from [1] and the vacuum oscillation probability, P_{vac} (black dots). The Middle panel is difference between exact oscillation probabilities in matter and vacuum (black dots), and the difference between exact and 0th DMP approximation (solid red) and exact and 1st DMP approximation (solid magenta) approximations. Bottom panel is similar to middle panel but plotting the fractional differences, $\Delta P/\overline{P}$. The density use is 3.0 g.cm^{-3}.

NOvA (810 km)

DUNE (1300 km)

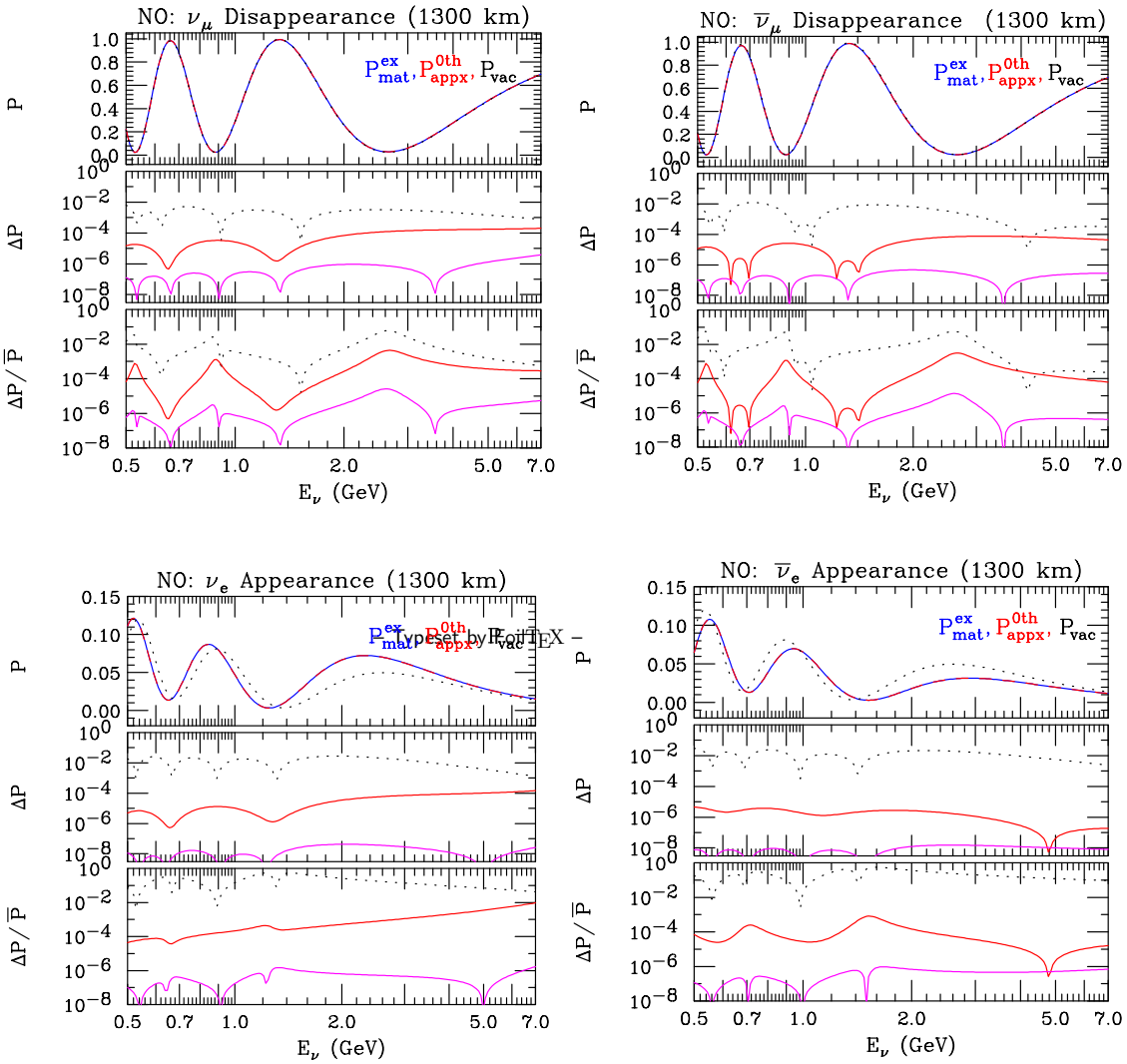

Top panel: P^{ex}_{mat}, P^{0th}_{appx} and P_{vac}

Middle and bottom panels:

black dotted lines	red solid lines	magenta solid lines
$\Delta P = \lvert P^{ex}_{mat} - P_{vac}\rvert$	$\Delta P = \lvert P^{ex}_{mat} - P^{0th}_{appx}\rvert$	$\Delta P = \lvert P^{ex}_{mat} - P^{1st}_{appx}\rvert$
$\overline{P} = \frac{1}{2}(P^{ex}_{mat} + P_{vac})$	$\overline{P} = \frac{1}{2}(P^{ex}_{mat} + P^{0th}_{appx})$	$\overline{P} = \frac{1}{2}(P^{ex}_{mat} + P^{1st}_{appx})$

Figure 9: DUNE, for normal ordering (NO): Top Left figure is ν_μ disappearance, Top Right figure is $\bar{\nu}_\mu$ disappearance, Bottom Left figure is $\nu_\mu \to \nu_e$ appearance, and Bottom Right is $\bar{\nu}_\mu \to \bar{\nu}_e$ appearance. In each figure, the top panel is exact oscillation probability in matter, P^{ex}_{mat} (blue dashes) from [3], the zeroth order DMP approximation, P^{0th}_{appx} (red dashes) from [1] and the vacuum oscillation probability, P_{vac} (black dots). The Middle panel is difference between exact oscillation probabilities in matter and vacuum (black dots), and the difference between exact and 0th DMP approximation (solid red) and exact and 1st DMP approximation (solid magenta) approximations. Bottom panel is similar to middle panel but plotting the fractional differences, $\Delta P/\overline{P}$. The density use is 3.0 g.cm^{-3}.

NOvA (810 km)

DUNE (1300 km)

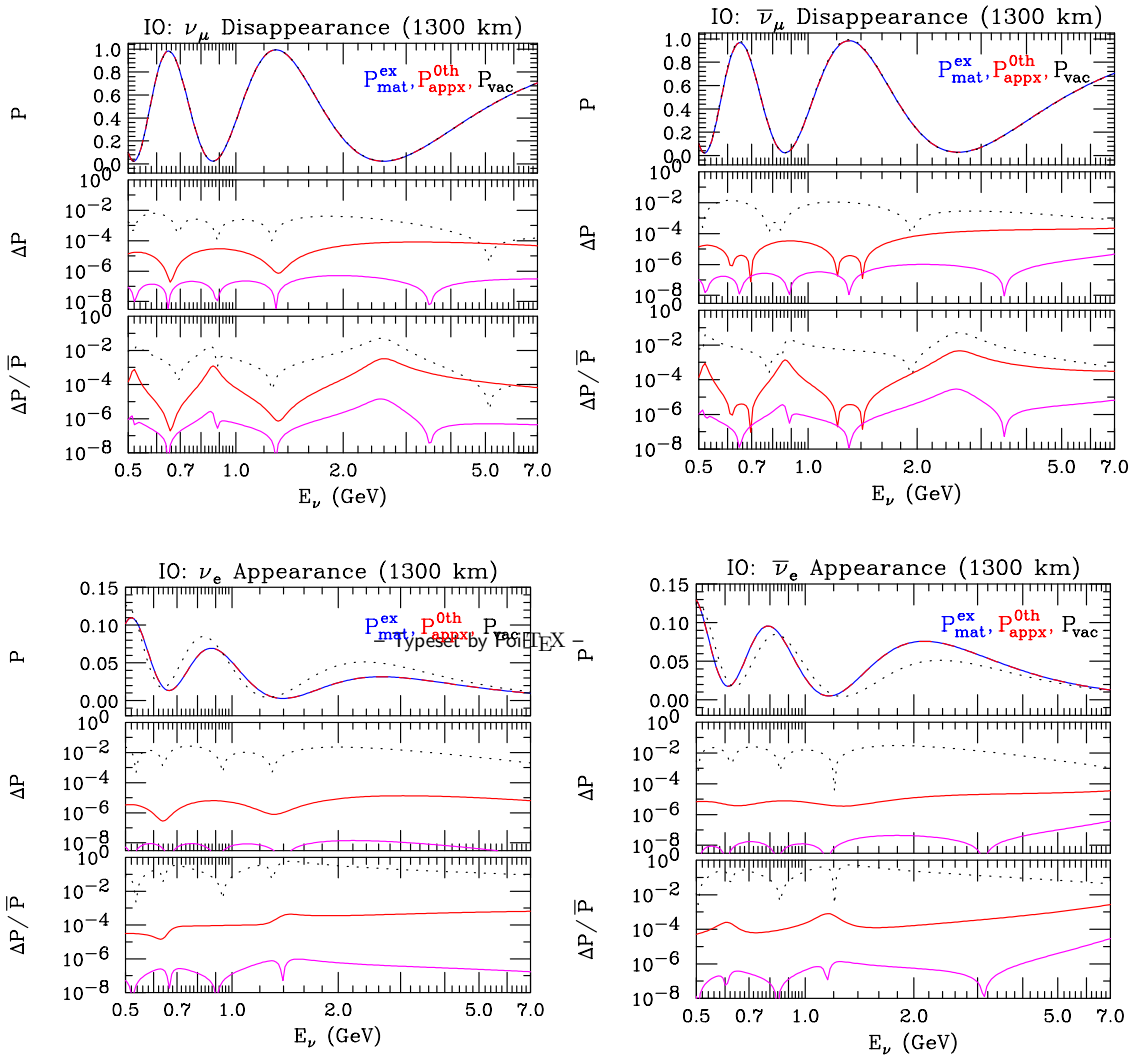

Top panel: P^{ex}_{mat}, P^{0th}_{appx} and P_{vac}

Middle and bottom panels:

black dotted lines	red solid lines	magenta solid lines
$\Delta P = \lvert P^{ex}_{mat} - P_{vac}\rvert$	$\Delta P = \lvert P^{ex}_{mat} - P^{0th}_{appx}\rvert$	$\Delta P = \lvert P^{ex}_{mat} - P^{1st}_{appx}\rvert$
$\overline{P} = \frac{1}{2}(P^{ex}_{mat} + P_{vac})$	$\overline{P} = \frac{1}{2}(P^{ex}_{mat} + P^{0th}_{appx})$	$\overline{P} = \frac{1}{2}(P^{ex}_{mat} + P^{1st}_{appx})$

Figure 10: DUNE, for inverted ordering (IO): Top Left figure is ν_μ disappearance, Top Right figure is $\bar{\nu}_\mu$ disappearance, Bottom Left figure is $\nu_\mu \to \nu_e$ appearance, and Bottom Right is $\bar{\nu}_\mu \to \bar{\nu}_e$ appearance. In each figure, the top panel is exact oscillation probability in matter, P^{ex}_{mat} (blue dashes) from [3], the zeroth order DMP approximation, P^{0th}_{appx} (red dashes) from [1] and the vacuum oscillation probability, P_{vac} (black dots). The Middle panel is difference between exact oscillation probabilities in matter and vacuum (black dots), and the difference between exact and 0th DMP approximation (solid red) and exact and 1st DMP approximation (solid magenta) approximations. Bottom panel is similar to middle panel but plotting the fractional differences, $\Delta P/\overline{P}$. The density use is 3.0 g.cm^{-3}.